

Analysis of a Step-Down DC-DC Converter: Linear Versus Nonlinear Circuit

Ioana-Gabriela Sîrbu*, Marius Voinea† and Mihai Iordache†

* University of Craiova, Faculty of Electrical Engineering, 107 Decebal Blvd., Craiova, Romania, osirbu@elth.ucv.ro

† Politehnica University of Bucharest, Faculty of Electrical Engineering, 313 Spl. Independentei, Bucharest, Romania, voineamarius@gmail.com, iordache@elth.pub.ro

Abstract - This paper aims to investigate the step-down dc-dc converters from circuit analysis viewpoint. These converters have a lot of utilizations, including different applications in power energy conversion domain, being mentioned also in electromagnetic compatibility studies. That is why the study and the analysis of such devices were and continue to be of a real interest for the scientific community. For this purpose this paper aims to bring a contribution in the domain, by offering equivalent schemes of different accuracies and alternative methods of analysis in time-varying regimes for step-down dc-dc converters used in electromagnetic compatibility investigations. Various time analysis methods are used here in order to analyze the step-down dc-dc converter circuit. Each method is well explained, starting from the basic equations of the circuit, continuing with the particularities of the approaches and finalizing with the presentation of the equations sets in the final form. For each method a program was created where the obtained equations were implemented. The most important results are presented in each case; they correspond both to the steady state and to the initial variable regime. The final part focuses on the differences between the results obtained using the real nonlinear characteristics of some elements and those resulted using their linearized model. The resulted waveforms are discussed comparatively not only using different methods of analysis and linear and nonlinear schemes of the converter, but also using results offered by commercial software specialized in electric and electronic circuit analysis. Finally the advantages and the disadvantages of each method are underlined and some conclusions are depicted.

Keywords: *circuit simulation, linear circuits, nonlinear circuits, time varying circuits, converters.*

I. INTRODUCTION

The dc-dc voltage converters are static switching electrical equipments that change the input constant dc voltage to an adjustable dc output voltage. The principal component responsible of this transformation is the electronic (semiconductor) switching element that changes its state from on to off. This switching element could be a GTO thyristor, an IGBT or a MOSFET transistor.

Because there is a small power loss inside these semiconductor elements, they achieve high energy conversion efficiency [1], [2]. As a consequence the power electronic switches are used to operate at high frequencies. Also the filter inductors and capacitors have smaller values.

The step-down dc-dc converter is commonly known as a buck converter. Among buck derived dc-dc converters, the most used are the forward converter, the push-pull converter, the half-bridge converter, and the full-bridge converter [1]. They are used in many applications such as: dc electric drives, dc power supplies (having the role of galvanic isolation), renewable dc sources, transportation systems and even in computer and telecommunication equipment [1]–[7]. Another area where the dc-dc converters are mentioned is the electromagnetic compatibility investigation. Taking the example of the power electronic loads, they pollute the supply grid with harmonics; that is why the dc-dc converters are used as intermediate stage to improve the power factor and to decrease the harmonic content.

The most popular type of dc-dc converters is the pulse width modulated converters [1], [2], [7]. Its advantages include high efficiency, simple control and relatively low component count. A disadvantage is due to the turn-on turn-off losses that limit operating frequencies to some hundreds of kilohertz.

The studies made in time on the dc-dc converters focused on finding new topologies, on developing improved solution in the converter production, but also on the analysis of their operation. For this purpose the circuit analysis of their equivalent diagrams played an important role [8]–[13].

In this paper a circuit analysis of a step-down dc-dc (buck) converter is made. The proposed analysis methods were applied on the linearized equivalent circuit of the converter, but also on the nonlinear variant of its diagram. For the linear circuit two methods were used: the state equation method and a mathematical method based on Kirchhoff's laws. For the nonlinear circuit, the circuit equations were brought to the form of a system that includes state equations and output equations. The final relations were implemented in MATLAB programs; their results were discussed comparatively. The advantages and the disadvantages of each approach are underlined. Finally our results were compared with the simulation results obtained using a software specialized in the electric circuit analysis (SPICE). The conclusions are formulated regarding the relation with previously published results of some researchers.

II. STEP-DOWN DC-DC CONVERTER WITH LINEAR PASSIVE COMPONENTS

We consider the case of a step-down dc-dc converter used in electromagnetic compatibility investigations. We

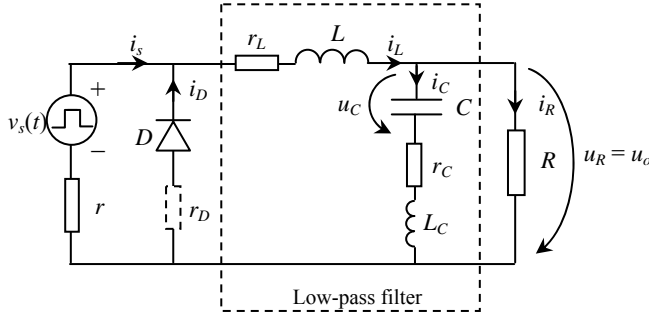


Fig. 1. Real step-down dc-dc converter diagram.

intend to take into account the energy dissipated in the passive elements, so - unlike previous works [1], [14] where ideal components were mainly considered - its equivalent electric circuit includes parasitic components (Fig. 1) [1]. The realistic model of the capacitor includes, besides its capacitance C , a series equivalent resistance r_C - due to the dielectric losses and the electrical connections - and a series inductance L_C of very small value that appear at high frequencies. The series inductance is rather important because it causes a limitation of the operating frequency [1]. The real coil has as parameters its inductance L , but also a series resistance r_L due mainly to the Joule losses in the conductive media.

For the diode D (considered here as linear element) we must consider its resistance r_D that varies function of its conductive state. It has a rather low value in the conduction state ($r_{D\text{on}} \approx 10^{-1} \Omega$) and a very high value in the blocked state ($r_{D\text{off}} \approx 10^6 \Omega$).

The dc voltage source and the switching (semiconductive) element were replaced in the diagram by a pulse voltage source $v_s(t)$. Its equivalent internal resistance has a small value, r (Fig. 1).

As for the load we considered only the case of a resistive load of value R because we are interested mainly in the model structure of the converter and its analysis method in time domain. After the validation of the model and the obtaining of valid results, it can be used in more complex schemes or for different types of consumers.

A. Circuit Analysis using the State Equation Method

Because the step-down dc-dc converter operates in a variable regime the most general approach that can be used is based on the state equation method. We can utilize it both for linear and nonlinear circuits, having the highest level of generality [8], [12], [13], [16]–[18].

In order to use state equation method for the circuit in Fig. 1 we must put the circuit equations in the general form [12], [13]:

$$\begin{cases} \dot{\mathbf{x}} = \mathbf{f}(\mathbf{x}, \mathbf{s}, t) \\ \mathbf{x}(t_0) = \mathbf{x}_0, \end{cases} \quad (1)$$

where \mathbf{x} is the state variables vector, \mathbf{s} is the sources vector and \mathbf{x}_0 is a vector that includes the values of the state variables at the initial moment t_0 .

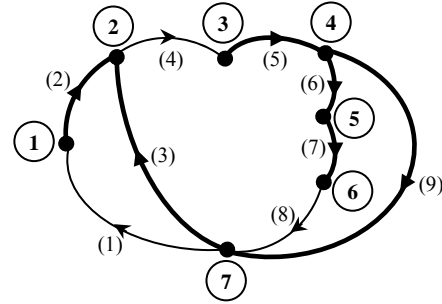


Fig. 2. The oriented graph of connexion for the converter circuit.

In our analysis we started from the topology of the circuit in Fig. 1. We establish for it the graph of connexion (Fig. 2).

Each node and each branch of the oriented graph was numbered. Consequently the subsequent study will use this numbering for the current and the voltage associated to each branch / element.

In the oriented graph we chose a normal tree that was marked in Fig. 2 with thick arcs. Its associated cotree is represented by thin arcs.

For this configuration we determined the essential incidence matrix \mathbf{D}_0 [12], [16], [17]:

$$\mathbf{D}_0 = \begin{matrix} & \begin{matrix} l_1 & l_4 & l_8 \end{matrix} \\ \begin{matrix} \Sigma_2 \\ \Sigma_3 \\ \Sigma_5 \\ \Sigma_6 \\ \Sigma_7 \\ \Sigma_9 \end{matrix} & \begin{pmatrix} -1 & 0 & 0 \\ 1 & -1 & 0 \\ 0 & -1 & 0 \\ 0 & 0 & -1 \\ 0 & 0 & -1 \\ 0 & -1 & 1 \end{pmatrix} \end{matrix}. \quad (2)$$

The lines of \mathbf{D}_0 were rearranged in the order of the element type situated on each branch, as: branches with resistors, branches with capacitances and branches with voltage sources. Thus we obtained the matrix \mathbf{D} that can be partitioned afterwards taking into account the different types of element on each branch [12]:

$$\mathbf{D} = \begin{matrix} & \begin{matrix} l_1 & l_4 & l_8 \end{matrix} \\ \begin{matrix} \Sigma_3 \\ \Sigma_5 \\ \Sigma_7 \\ \Sigma_9 \\ \Sigma_6 \\ \Sigma_2 \end{matrix} & \begin{pmatrix} 1 & -1 & 0 \\ 0 & -1 & 0 \\ 0 & 0 & -1 \\ 0 & -1 & 1 \\ 0 & 0 & -1 \\ -1 & 0 & 0 \end{pmatrix} \end{matrix} = \begin{pmatrix} \mathbf{D}_{RR} & \mathbf{D}_{RL} \\ \mathbf{D}_{CR} & \mathbf{D}_{CL} \\ \mathbf{D}_{ER} & \mathbf{D}_{EL} \end{pmatrix}. \quad (3)$$

Based on matrix \mathbf{D} we can write the tree branches currents as function of cotree branches currents:

$$\mathbf{i}_t = -\mathbf{D} \cdot \mathbf{i}_c, \quad (4)$$

where

$$\mathbf{i}_t = (i_3 \ i_5 \ i_7 \ i_9 \ i_6 \ i_2)^t = (\mathbf{i}_{Rt} \ \mathbf{i}_C \ \mathbf{i}_E)^t$$

$$\mathbf{i}_c = (i_1 \ i_4 \ i_8)^t = (\mathbf{i}_{Rc} \ \mathbf{i}_L)^t,$$

and the cotree branches voltages as function of the tree branches voltages:

$$\mathbf{u}_c = \mathbf{D}^t \cdot \mathbf{u}_t, \quad (5)$$

where

$$\mathbf{u}_c = (u_1 \quad u_4 \quad u_8)^t = (\mathbf{u}_{Rc} \quad \mathbf{u}_L)^t$$

$$\mathbf{u}_t = (u_3 \quad u_5 \quad u_7 \quad u_9 \quad u_6 \quad u_2)^t = (\mathbf{u}_{Rt} \quad \mathbf{u}_C \quad \mathbf{u}_E)^t$$

In the relations (4) and (5) if we consider only the branches with resistances [12], we can write that:

$$\mathbf{i}_{Rt} + \mathbf{D}_{RR} \cdot \mathbf{i}_{Rc} + \mathbf{D}_{RL} \cdot \mathbf{i}_L = \mathbf{0}_{4 \times 1}, \quad (6)$$

$$\mathbf{u}_{Rc} - \mathbf{D}_{RR}^t \cdot \mathbf{u}_{Rt} - \mathbf{D}_{CR}^t \cdot \mathbf{u}_C + \mathbf{D}_{ER}^t \cdot \mathbf{e} = \mathbf{0}_{1 \times 1} \quad (7)$$

with $\mathbf{e} = -\mathbf{u}_E = \mathbf{v}_s(t)$.

These relations are completed with the equations specific to the resistive branches:

$$\begin{aligned} \mathbf{i}_{Rt} &= \mathbf{G}_t \cdot \mathbf{u}_{Rt} \\ \mathbf{u}_{Rc} &= \mathbf{R}_c \cdot \mathbf{i}_{Rc}, \end{aligned} \quad (8)$$

where

$$\mathbf{G}_t = \begin{pmatrix} 1/r_D & 0 & 0 & 0 \\ 0 & 1/r_L & 0 & 0 \\ 0 & 0 & 1/r_C & 0 \\ 0 & 0 & 0 & 1/R \end{pmatrix} \text{ and } \mathbf{R}_c = r.$$

The relations (8) replace the correspondent terms from (6) and (7), obtaining

$$\begin{aligned} \mathbf{G}_t \cdot \mathbf{u}_{Rt} + \mathbf{D}_{RR} \cdot \mathbf{i}_{Rc} &= -\mathbf{D}_{RL} \cdot \mathbf{i}_L \\ -\mathbf{D}_{RR}^t \cdot \mathbf{u}_{Rt} + \mathbf{R}_c \cdot \mathbf{i}_{Rc} &= \mathbf{D}_{CR}^t \cdot \mathbf{u}_C - \mathbf{D}_{ER}^t \cdot \mathbf{e} \end{aligned} \quad (9)$$

or, in matrix form,

$$\begin{pmatrix} \mathbf{G}_t & \mathbf{D}_{RR} \\ -\mathbf{D}_{RR}^t & \mathbf{R}_c \end{pmatrix} \cdot \begin{pmatrix} \mathbf{u}_{Rt} \\ \mathbf{i}_{Rc} \end{pmatrix} = \begin{pmatrix} \mathbf{0} & -\mathbf{D}_{RL} \\ \mathbf{D}_{CR}^t & \mathbf{0} \end{pmatrix} \cdot \begin{pmatrix} \mathbf{u}_C \\ \mathbf{i}_L \end{pmatrix} - \begin{pmatrix} \mathbf{0} \\ \mathbf{D}_{ER}^t \end{pmatrix} \cdot \mathbf{e}.$$

In the equations (4) and (5) we consider now only the branches with capacitances and inductances

$$\mathbf{i}_C = -\mathbf{D}_{CR} \cdot \mathbf{i}_{Rc} - \mathbf{D}_{CL} \cdot \mathbf{i}_L \quad (10)$$

$$\mathbf{u}_L = \mathbf{D}_{RL}^t \cdot \mathbf{u}_{Rt} + \mathbf{D}_{CL}^t \cdot \mathbf{u}_C + \mathbf{D}_{EL}^t \cdot \mathbf{u}_E \quad (11)$$

or in matrix form [12]

$$\begin{pmatrix} \mathbf{i}_C \\ \mathbf{u}_L \end{pmatrix} + \begin{pmatrix} \mathbf{0} & \mathbf{D}_{CR} \\ -\mathbf{D}_{RL}^t & \mathbf{0} \end{pmatrix} \cdot \begin{pmatrix} \mathbf{u}_{Rt} \\ \mathbf{i}_{Rc} \end{pmatrix} = \begin{pmatrix} \mathbf{0} & -\mathbf{D}_{CL} \\ \mathbf{D}_{CL}^t & \mathbf{0} \end{pmatrix} \cdot \begin{pmatrix} \mathbf{u}_C \\ \mathbf{i}_L \end{pmatrix} - \begin{pmatrix} \mathbf{0} \\ \mathbf{D}_{EL}^t \end{pmatrix} \cdot \mathbf{e}$$

These relations are completed with the equations of evolution for capacitances and inductances

$$\begin{pmatrix} \mathbf{i}_C \\ \mathbf{u}_L \end{pmatrix} = \begin{pmatrix} \mathbf{C} & \mathbf{0} \\ \mathbf{0} & \mathbf{L} \end{pmatrix} \cdot \begin{pmatrix} \dot{\mathbf{u}}_C \\ \dot{\mathbf{i}}_L \end{pmatrix} \Leftrightarrow \begin{pmatrix} \mathbf{i}_C \\ \mathbf{u}_L \end{pmatrix} = \begin{pmatrix} \mathbf{C} & \mathbf{0} & \mathbf{0} \\ \mathbf{0} & \mathbf{L} & \mathbf{0} \\ \mathbf{0} & \mathbf{0} & \mathbf{L}_C \end{pmatrix} \cdot \begin{pmatrix} \dot{\mathbf{u}}_6 \\ \dot{\mathbf{i}}_4 \\ \dot{\mathbf{i}}_8 \end{pmatrix} \quad (12)$$

By replacing (9) and (12) in (10) and (11) we obtain the state equations in the form

$$\begin{cases} \dot{\mathbf{x}} = \mathbf{M} \cdot \mathbf{x} + \mathbf{N} \cdot \mathbf{e} \\ \mathbf{x}(0) = \mathbf{0}, \end{cases} \quad (13)$$

where

$$\mathbf{x} = (u_6 \quad i_4 \quad i_8)^t$$

$$\mathbf{M} = \begin{pmatrix} \mathbf{C} & \mathbf{0} \\ \mathbf{0} & \mathbf{L} \end{pmatrix}^{-1} \cdot \left[-\begin{pmatrix} \mathbf{0} & \mathbf{D}_{CR} \\ -\mathbf{D}_{RL}^t & \mathbf{0} \end{pmatrix} \cdot \begin{pmatrix} \mathbf{G}_t & \mathbf{D}_{RR} \\ -\mathbf{D}_{RR}^t & \mathbf{R}_c \end{pmatrix}^{-1} \cdot \begin{pmatrix} \mathbf{0} & -\mathbf{D}_{RL} \\ \mathbf{D}_{CR}^t & \mathbf{0} \end{pmatrix} + \begin{pmatrix} \mathbf{0} & -\mathbf{D}_{CL} \\ \mathbf{D}_{CL}^t & \mathbf{0} \end{pmatrix} \right] \text{ and}$$

$$\mathbf{N} = \begin{pmatrix} \mathbf{C} & \mathbf{0} \\ \mathbf{0} & \mathbf{L} \end{pmatrix}^{-1} \cdot \left[\begin{pmatrix} \mathbf{0} & \mathbf{D}_{CR} \\ -\mathbf{D}_{RL}^t & \mathbf{0} \end{pmatrix} \cdot \begin{pmatrix} \mathbf{G}_t & \mathbf{D}_{RR} \\ -\mathbf{D}_{RR}^t & \mathbf{R}_c \end{pmatrix}^{-1} \cdot \begin{pmatrix} \mathbf{0} \\ \mathbf{D}_{ER}^t \end{pmatrix} - \begin{pmatrix} \mathbf{0} \\ \mathbf{D}_{EL}^t \end{pmatrix} \right].$$

For our circuit

$$\mathbf{M} = \begin{pmatrix} 0 & 0 & 1/C \\ 0 & R_e/L & R/L \\ -1/L_C & R/L_C & -(R+r_C)/L_C \end{pmatrix} \quad (14)$$

$$\mathbf{N} = (0 \quad (r_D/L)/(r+r_D) \quad 0)^t \quad (15)$$

with $R_e = -r \cdot r_D / (r+r_D) - r_L - R$.

We implemented the differential system (13) in a MATLAB program [15] in order to verify the efficiency of the method. The circuit parameters we considered are: $r = 0.1 \Omega$, $L = 75 \mu\text{H}$, $C = 25 \mu\text{F}$, $R = 10 \Omega$, $r_L = 0.1 \Omega$, $r_C = 0.02 \Omega$, $L_C = 10 \mu\text{H}$, $f = 100 \text{ kHz}$, $D_r = 0.5$ (the duty ratio at the pulse equivalent source), $r_{D\text{on}} = 0.4574 \Omega$ and $r_{D\text{off}} = 10^6 \Omega$. They correspond to possible values of those parameters of a step-down dc-dc converter used in electromagnetic compatibility studies [19]–[21]. Some results are presented in Figs. 3–8.

Fig. 3 presents the variation in time of the voltage $u_6 = u_C$ at the capacitance terminals. One can observe that the steady state is obtained after 1.6 ms. The oscillations during the transient regime are not greater than 9.1V, i.e. 57% over the mean value of the voltage during the steady state.

Fig. 4 shows the same voltage in steady state. One can notice a very good limitation of the ripples; the peak-to-peak value is of only 16 mV that represents only around 2.7% of this voltage mean value.

Fig. 5 shows the variation in time of the current $i_4 = i_L$ through the coil. One can remark that the steady state is obtained after 1.6 ms (as in Fig. 3). The oscillations during the transient regime reach the value of 3.15 A, that means they can be five times bigger than the mean value of the current during the steady state.

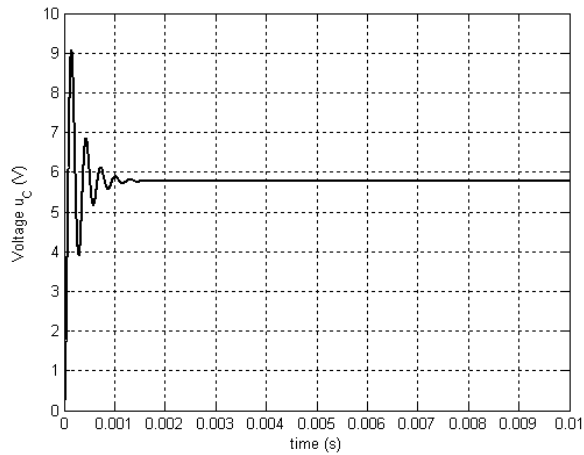
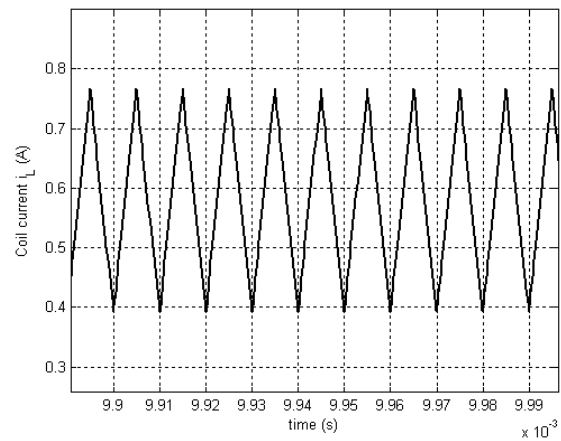
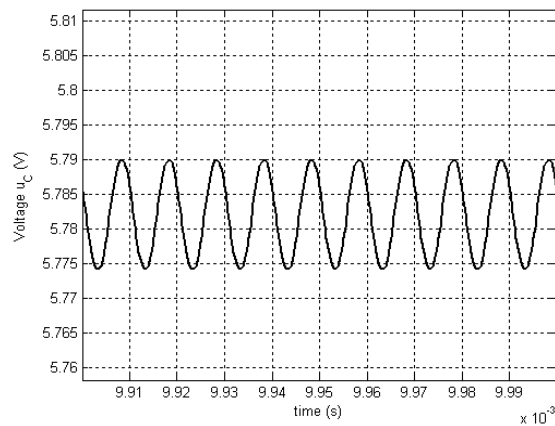
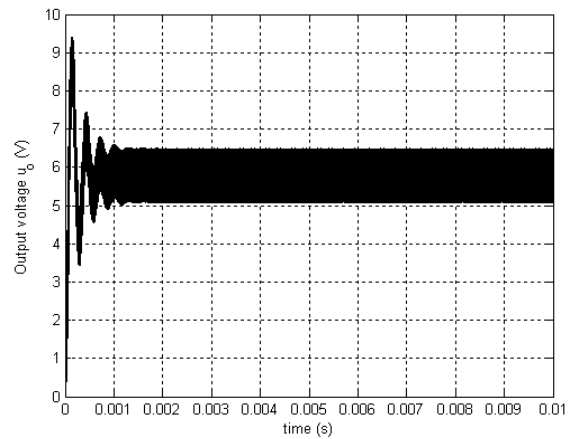
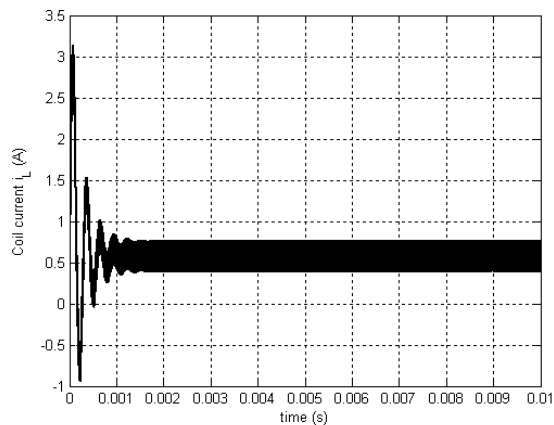
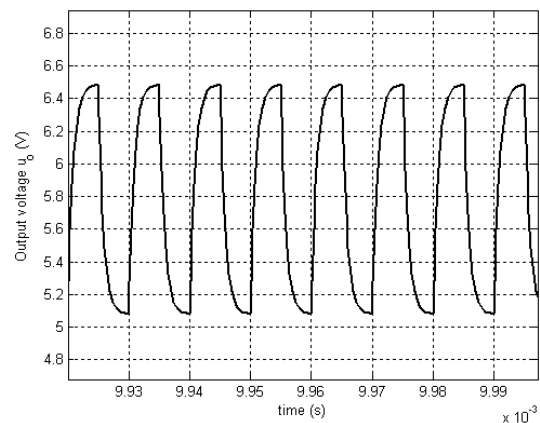
Fig. 3. Time variation of the capacitance voltage u_C .Fig. 6. Inductance current i_4 in steady state.Fig. 4. Capacitance voltage u_C in steady state.Fig. 7. Time variation of the load voltage u_9 .Fig. 5. Time variation of the inductance current i_4 .

Fig. 6 presents the same current in steady state. One can notice that the peak-to-peak value is 0.35 A while the current mean value is 0.58 A.

Fig. 7 presents the variation in time of the voltage $u_9 = u_o$ at the resistive load terminals. One can make the same observation that the steady state is obtained after 1.6 ms.

Fig. 8. Load voltage u_9 in steady state.

The oscillations during the transient regime are not greater than 9.3V, i.e. 60% over the mean value of the voltage during the steady state. Fig. 8 shows the same voltage in steady state. One can notice that the peak-to-peak value is of 1.38 V that represents around 23.7% of this voltage mean value.

By comparing the shape of the waveforms with those presented in the technical literature [1]–[3] we could

remark that they are similar. This fact proves that the circuit analysis using the state equation method was well done.

In what concerns the time variation of the electrical quantities obtained here we must put the question if they represent precisely their variation during the transient regime or they are influenced by the convergence of the numerical procedure. That is why we decided to use an alternative method of analysis for the step-down dc-dc converter linearized circuit.

B. Circuit Analysis Using a Mathematical Method Based on Kirchhoff's Laws

We started from the same step-down dc-dc converter diagram presented in Fig. 1. By applying the Kirchhoff's laws to this circuit we obtained:

$$\begin{aligned} r \cdot i_s - r_D \cdot i_D &= v_s \\ L \cdot di_L / dt + r_L i_L + L_C \cdot di_C / dt + r_C i_C + u_C + r_D i_D &= 0 \\ R \cdot i_R - u_C - r_C \cdot i_C - L_C \cdot di_C / dt &= 0 \\ i_s + i_D - i_L &= 0 \\ i_L - i_C - i_R &= 0 \end{aligned} \quad (16)$$

This system is completed with the relation between the current and the voltage of the capacitor C:

$$i_C = C \cdot du_C / dt. \quad (17)$$

By applying successive substitutions we obtained a differential equation with the unknown variable u_C [14]:

$$a \cdot \frac{d^3 u_C}{dt^3} + b \cdot \frac{d^2 u_C}{dt^2} + c \cdot \frac{du_C}{dt} + d \cdot u_C = e, \quad (18)$$

where

$$\begin{aligned} a &= L \cdot L_C \cdot C / R, \\ b &= C \cdot (L + L_C + L r_C / R + r_L L_C / R) + C \cdot (r_D r L_C / R) \cdot \\ &\quad \cdot 1 / (r + r_D), \\ c &= C \cdot (r_C + r_L + r_D \cdot r / (r + r_D)) + C \cdot (r_D r \cdot r_C / R) \cdot \\ &\quad \cdot 1 / (r + r_D) + C \cdot r_L r_C / R + L / R, \\ d &= 1 + (1 / R) \cdot (r_L + r_D r / (r + r_D)), \\ e &= v_s \cdot r_D / (r + r_D). \end{aligned}$$

Using the notation $y = u_C$, the differential equation (18) takes the form [14]

$$a \cdot y^{(3)} + b \cdot y^{(2)} + c \cdot y^{(1)} + d \cdot y = e, \quad (19)$$

with

$$\begin{aligned} y(0) &= v_s \cdot r_D / (r + r_D) = e, \\ y^{(1)}(0) &= 0, \\ y^{(2)}(0) &= 0. \end{aligned}$$

The differential equation of order 3 (19) can be replaced by a system of equations of order 1 [14], [15]. Thus (19) can be written as

$$y^{(3)} = -\frac{b}{a} \cdot y^{(2)} - \frac{c}{a} \cdot y^{(1)} - \frac{d}{a} \cdot y + \frac{e}{a}, \quad (20)$$

and with the notations

$$\begin{aligned} y_1 &= y^{(2)} \\ y_2 &= y^{(1)} \\ y_3 &= y \end{aligned} \quad (21)$$

the differential equation (19) is transformed into the system (22):

$$\begin{cases} y_1^{(1)} = -\frac{b}{a} \cdot y_1 - \frac{c}{a} \cdot y_2 - \frac{d}{a} \cdot y_3 + \frac{e}{a} \\ y_2^{(1)} = y_1 \\ y_3^{(1)} = y_2 \end{cases} \quad (22)$$

For the system (22) we implemented a Runge-Kutta method of third order in a MATLAB function [15] and thus we obtained the variation of the capacitance voltage u_C and afterwards the output voltage u_o and coil current i_L (other electric quantities could be determined if it is desired).

By keeping the same values for the circuit parameters we obtained the results presented in Figs. 9 – 13.

Fig. 9 presents the variation in time of the voltage u_C at the capacitance terminals, obtained using the second method of analysis. One can observe that the steady state is obtained in less than 2.5 ms. The oscillations peaks obtained during the transient regime are not greater than 6.15V, i.e. 6.3 % over the mean value of the voltage during the steady state. This fact shows a different behavior during the first 2.5 ms by comparing with the result obtain using the state equation method.

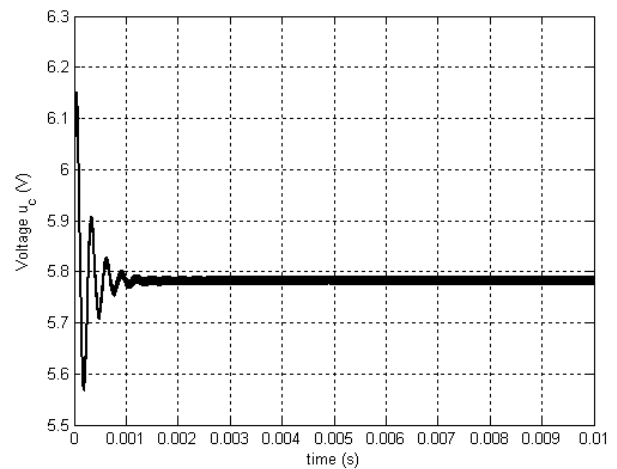
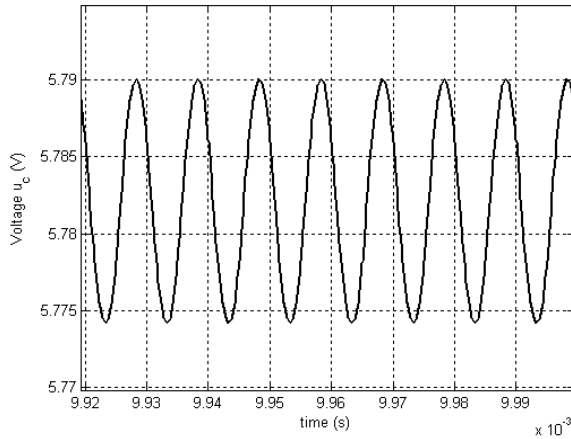
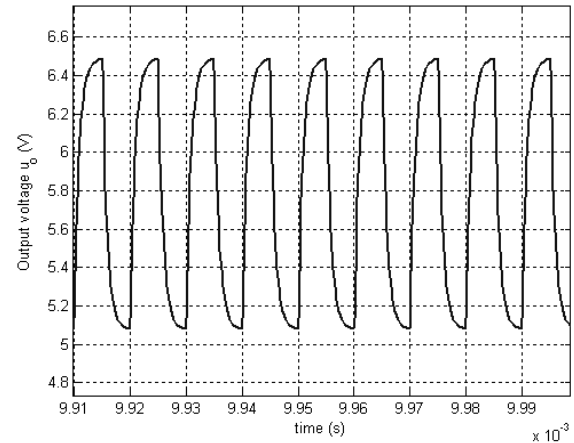
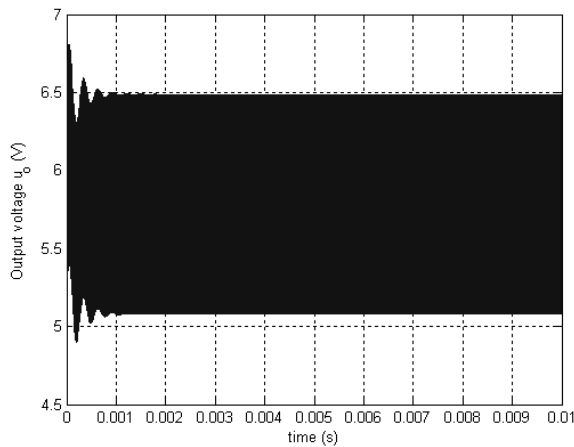
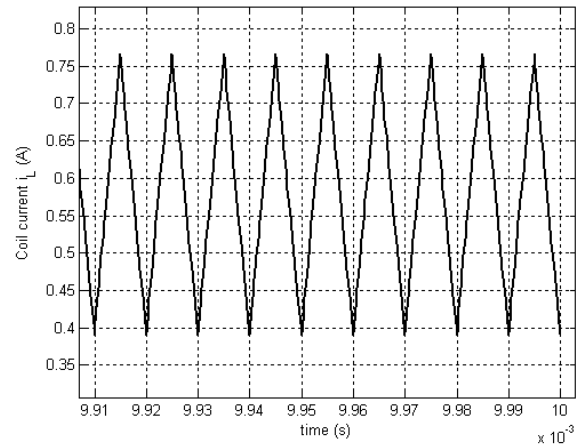


Fig. 9. Time variation of the capacitance voltage u_C .

Fig. 10. Capacitance voltage u_C in steady state.Fig. 12. Load voltage u_o in steady stateFig. 11. Time variation of the load voltage u_o .Fig. 13. Inductance current i_L in steady state.

These different results show that the numerical method used in solving the same electric circuit influences the time variation of the electric quantity. Thus in the first 2.5 ms we observe not only the transient regime but also information on the stability and the convergence of the numerical procedure. From this viewpoint we concluded that the second method that uses a mathematical method based on Kirchhoff's law for the circuit analysis improves the numerical stability, offering lower peaks in the initial transition interval.

Fig. 10 shows the same voltage in steady state. One can notice that this result is similar to that one depicted in Fig. 4. So we concluded that the results in steady state are not influenced by the chosen method.

Fig. 11 presents the variation in time of the voltage u_o at the resistive load terminals. One can make the observation that the steady state is obtained after 1.1 ms.

The oscillations during the transient regime are not greater than 6.8V, i.e. 17.2 % over the mean value of the voltage during the steady state. This confirms the above conclusion that there is a different behavior during the first 2 ms by comparing with the result obtained using the state equation method and that the second method improves the numerical stability, offering lower peaks in the transition interval.

Fig. 12 shows the same voltage u_o in steady state. This result is similar to those depicted in Fig. 8, obtained using the first method.

Fig. 13 presents the current through the coil i_L in steady state. Also in this case the waveform is similar to those obtained using the state equation method (Fig. 6).

III. STEP-DOWN DC-DC CONVERTER WITH NONLINEAR PASSIVE COMPONENTS

In this part we consider the same general diagram in Fig. 1. However the diode is treated in a realistic manner, i.e. as a nonlinear element. Because it is characterized by a nonlinear current-voltage dependence, the diode can be symbolized as a nonlinear conductance (Fig. 14). By applying the Kirchhoff's laws in this circuit we obtained:

$$\begin{aligned}
 r \cdot i_s - u_D &= v_s \\
 L \cdot di_L / dt + r_L i_L + L_C \cdot di_C / dt + r_C i_C + u_C + u_D &= 0 \\
 R \cdot i_R - u_C - r_C \cdot i_C - L_C \cdot di_C / dt &= 0 \\
 i_s + i_D - i_L &= 0 \\
 i_L - i_C - i_R &= 0
 \end{aligned} \tag{23}$$

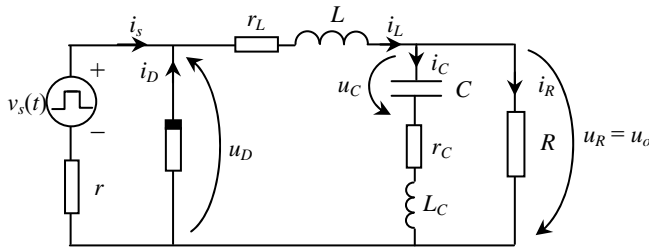


Fig. 14. Nonlinear step-down dc-dc converter diagram.

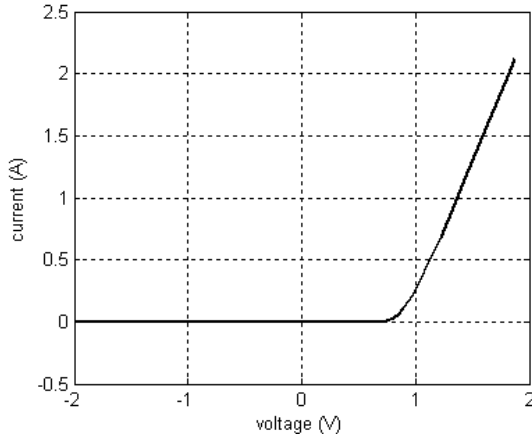


Fig. 15. Nonlinear current-voltage characteristic of the diode.

The system (23) is completed by the relation between the current and the voltage of the capacitor C (17) and by the nonlinear current-voltage dependence of the nonlinear element, i.e. the diode (Fig. 15):

$$i_D = i_D(u_D). \quad (24)$$

In order to be solved, the system of equations (17), (23), (24) is brought to the general form [12], [13]:

$$\begin{cases} \dot{\mathbf{x}} = \mathbf{f}(\mathbf{x}, \mathbf{y}, \dot{\mathbf{s}}, \mathbf{s}, t), & \mathbf{x}(t_0) = \mathbf{x}_0, \\ \mathbf{y} = \mathbf{g}(\mathbf{x}, \mathbf{s}, t), \end{cases} \quad (25)$$

that includes state equations and output equations. \mathbf{x} is the state variables vector, \mathbf{y} is the output variables vector, \mathbf{s} is the sources vector and \mathbf{x}_0 is a vector that includes the values of the variables at the initial moment t_0 .

Thus the system becomes:

$$\begin{cases} du_C / dt = 1/C \cdot i_C \\ di_L / dt = -(r_L + R)/L \cdot i_L + R/L \cdot i_C - 1/L \cdot u_D \\ di_C / dt = -1/L_C \cdot u_C + R/L_C \cdot i_L - (R + r_C)/L_C \cdot i_C \\ u_D = r/(1 + r \cdot g_d) \cdot (i_L - 1/r \cdot v_s - j_0), \end{cases} \quad (26)$$

where we treated the nonlinear element as a voltage controlled nonlinear resistor with a locally linearized characteristic: g_d is its dynamic conductance in the operating point and j_0 is its correspondent ideal current source [8], [12], [13].

Making a correspondence between the systems (26) and (25),

$$\mathbf{x} = \begin{pmatrix} u_C \\ i_L \\ i_C \end{pmatrix}, \quad \mathbf{x}(t_0) = \mathbf{x}(0) = \begin{pmatrix} 0 \\ 0 \\ 0 \end{pmatrix}, \quad \mathbf{s} = v_s, \quad \mathbf{y} = u_D, \quad (27)$$

and (26) is written as

$$\begin{cases} \dot{\mathbf{x}} = \mathbf{A} \cdot \mathbf{x} + \mathbf{B} \cdot \mathbf{y} \\ \mathbf{y} = \mathbf{C} \cdot \mathbf{x} + \mathbf{D} \cdot \mathbf{s} + \mathbf{E} \\ \mathbf{x}(0) = \mathbf{0}_{3 \times 1} \end{cases} \quad (28)$$

where

$$\mathbf{A} = \begin{pmatrix} 0 & 0 & 1/C \\ 0 & -(r_L + R)/L & R/L \\ -1/L_C & R/L_C & -(R + r_C)/L_C \end{pmatrix},$$

$$\mathbf{B} = (0 \quad -1/L \quad 0)^T,$$

$$\mathbf{C} = (0 \quad r/(1 + r \cdot g_d) \quad 0)^T,$$

$$\mathbf{D} = -1/(1 + r \cdot g_d), \text{ and}$$

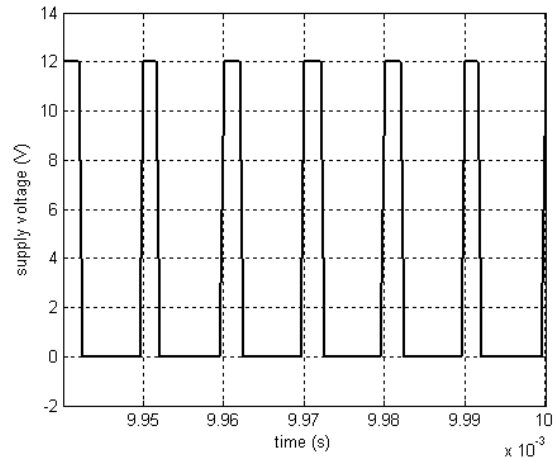
$$\mathbf{E} = -r \cdot j_0 / (1 + r \cdot g_d).$$

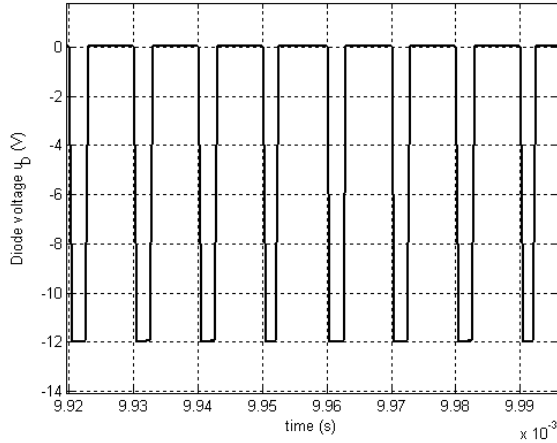
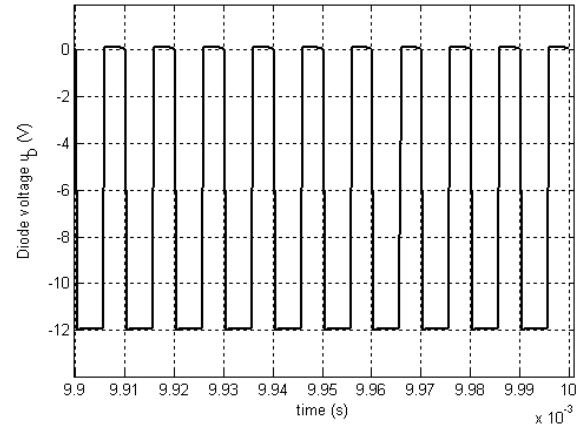
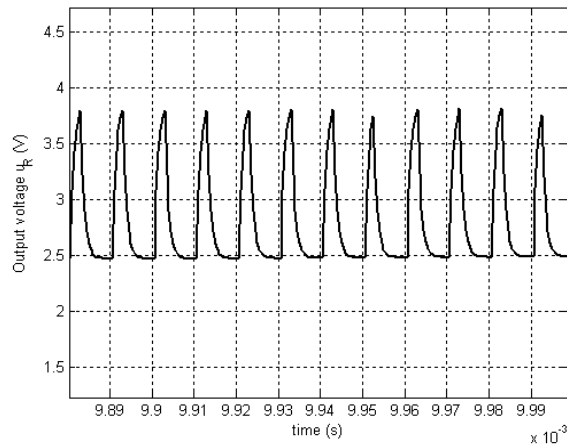
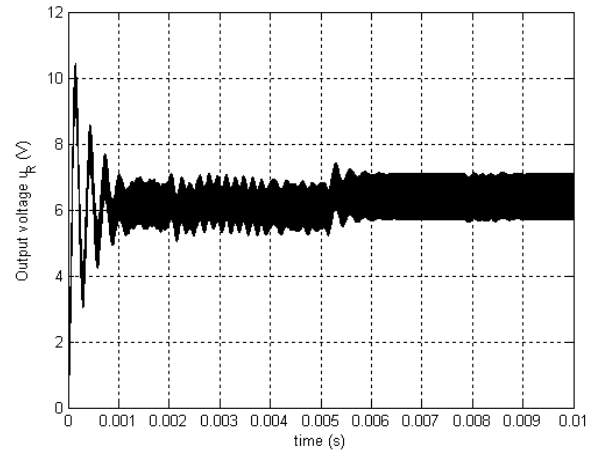
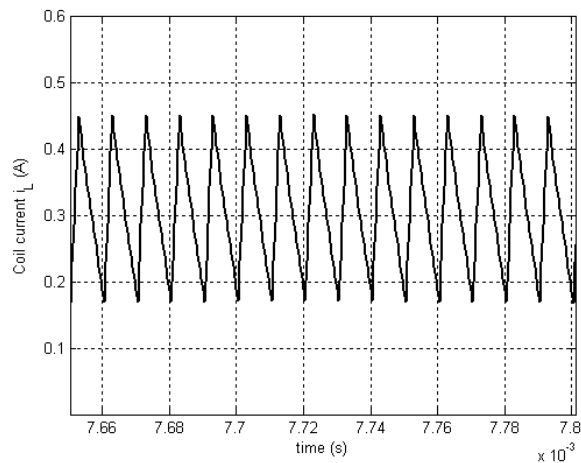
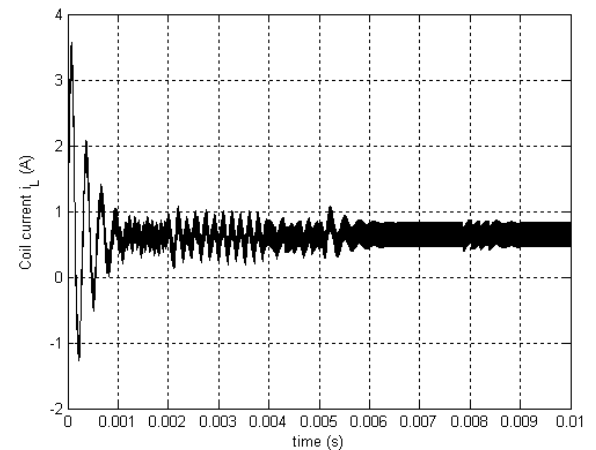
The equations (28) are solved numerically for each time step. The two types of equations (state equations and output equations) are solved alternately [12], [13]. Firstly the output equation is solved for a given value of \mathbf{x} (e.g. initial conditions \mathbf{x}_0); then for the next time interval the state equations are integrated numerically, using the value of \mathbf{y} previously calculated. These two steps repeat consecutively until the entire time interval of analysis is covered.

This algorithm was implemented in a MATLAB program. For the parameters of the circuit we chose the same values as above. As diode we used a 1N916 type diode. Its characteristic was depicted in Fig. 15.

Firstly a duty ratio D_r of 0.2 was considered. The pulse supply voltage and the obtained diode voltage are depicted in Fig. 16 and Fig. 17 respectively.

The load voltage u_o and the coil current i_L obtained in this case (for steady state) are presented in Fig. 18 and Fig. 19 respectively.

Fig. 16. The pulsed supply voltage $v_s(t)$ for the duty ratio of 0.2.

Fig. 17. The diode voltage u_D for the duty ratio of 0.2.Fig. 20. The diode voltage u_D for the duty ratio of 0.5.Fig. 18. The load voltage u_o in steady state for the duty ratio of 0.2.Fig. 21. The time variation of the load voltage u_o for the duty ratio of 0.5.Fig. 19. The inductance current i_L in steady state for the duty ratio of 0.2.Fig. 22. The time variation of the coil current i_L for the duty ratio of 0.5.

Because the supplying interval is much small, the waveforms obtained for $D_r = 0.2$ are different comparative with those obtained for $D_r = 0.5$. If the coil current is different only in what concerns the slope in 'on' and in 'off' mode, the output voltage u_o has a pointed

form that suggests a more important influence of the higher order harmonics and consequently a worsening in the power quality. Of course, because the duty ratio is lower, the mean value of the electrical quantities are lower than for $D_r = 0.5$.

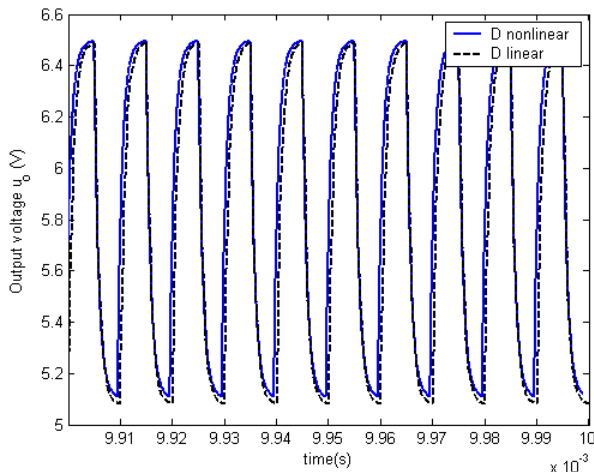


Fig. 23. Comparative waveforms for the load voltage u_o in steady state for the duty ratio of 0.5: nonlinear characteristic of the diode vs. linearized characteristic of the diode.

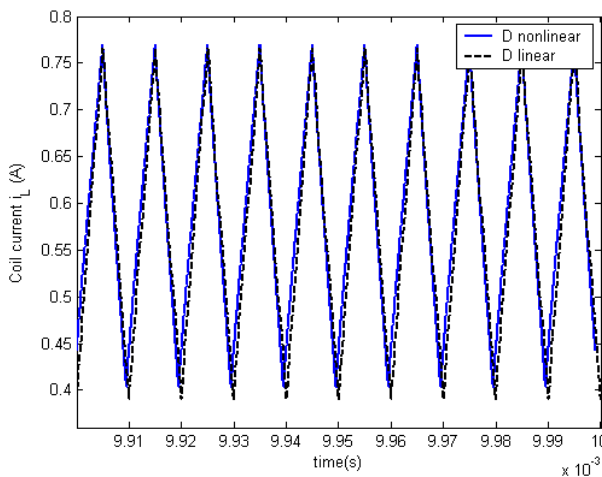


Fig. 24. Comparative waveforms for the coil current i_L in steady state for the duty ratio of 0.5: nonlinear characteristic of the diode vs. linearized characteristic of the diode.

Returning to the case of $D_r = 0.5$ we can proceed to a comparative analysis of the electrical quantities variations.

Fig. 20 presents the resulted time variation of the diode voltage for the duty ratio of 0.5. One can notice that the 'on' and 'off' intervals are equal and correspond to the pulses offered by the supply source voltage.

Analyzing the time variation of the load voltage (Fig. 21) we observed that in this case the instability interval last longer, around 9 ms. This is caused especially by the nonlinearity of the diode characteristic. Also in this interval the oscillation peaks are higher comparative to those obtained in the linearized model previously presented, reaching the value of 10.2 V, i.e. 75.8 % higher than the mean value in steady state.

Similar observations can be made on the time variation of the coil current (Fig. 22). In this case the oscillation peaks reached the value of 3.6 A, i.e. six times higher than the mean value in steady state.

Figs. 23 and 24 present in a comparative manner the load voltage u_o and the coil current i_L obtained in steady

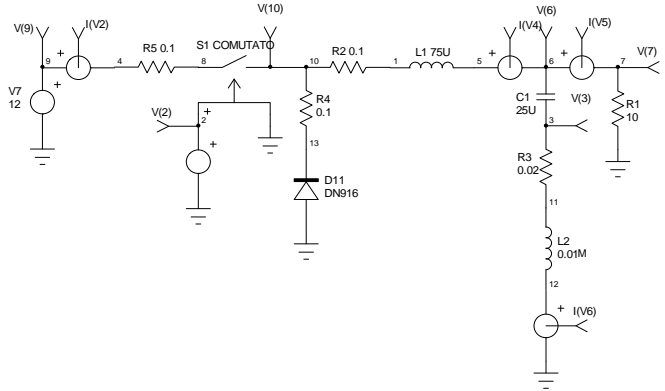


Fig. 25. SPICE model of the step-down dc-dc converter circuit.

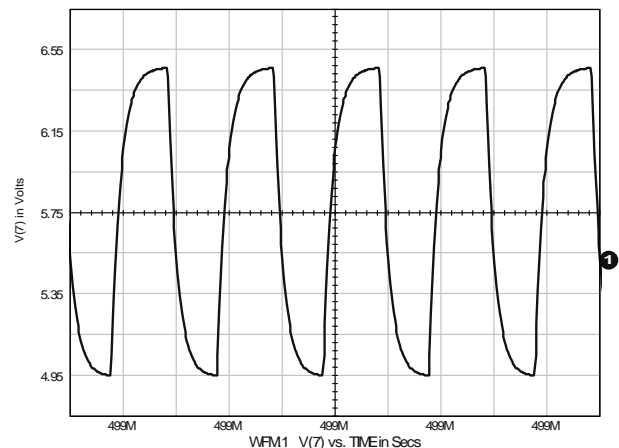


Fig. 26. The load voltage u_o in steady state for the duty ratio of 0.5 and using the nonlinear characteristic of the diode (SPICE result).

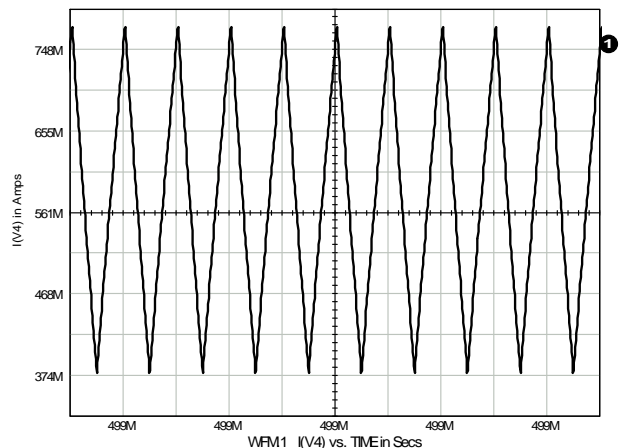


Fig. 27. The coil current i_L in steady state for the duty ratio of 0.5 and using the nonlinear characteristic of the diode (SPICE result).

state in the cases when the nonlinear current-voltage characteristic of the diode and its linearized characteristic were considered respectively. One can notice that these waveforms are almost the same, the differences between them being rather small. Although by considering the nonlinear $i-u$ dependence the results are more exact, the linearized form can be used successfully in the circuit

analysis of the step-down dc-dc converter with very good results and with a rather short computation time.

In order to validate the results obtained using our own programs we realized a simulation of the system using a commercial program (SPICE) (Fig. 25). Here the nonlinear characteristic of the diode was considered, the properties of this element imported from the program library being used [19].

Some of the simulated results are presented in Figs. 26 and 27. Fig. 26 shows the waveform of the load voltage u_o in steady state regime. Also the simulated coil current i_L is depicted in Fig. 27.

For a better comparative analysis of the waveforms obtained using our nonlinear model of the step-down dc-dc converter (simulated in a MATLAB program) and the program SPICE, the correspondent quantities were represented in the same diagram (Fig. 28 and Fig. 29).

One can notice that the results obtained in SPICE are identically with those obtained using the state equation for the nonlinear model, implemented in a MATLAB program. In Fig. 28 and in Fig. 29, where the load voltage u_o and the coil current i_L are represented respectively, the two waveforms are overlapped.

Comparing the results obtained in MATLAB for the nonlinear model of the step-down dc-dc converter firstly with its linear model (Fig. 23 and Fig 24) and then with the results provided by a commercial specialized program - considered as reference (Fig. 28 and Fig. 29) we could verify on the one hand the correctness of the problem solving and of the implemented programs, and on the other hand the deviations that are introduced by a linearized model of the converter (in this case minor deviations resulted and they could be neglected). The shape of the obtained curves corresponds also, in qualitative terms, to the results obtained by various researchers [1]–[3].

IV. CONCLUSION

This study realized a complete analysis of the step-down dc-dc converter from electrical circuit viewpoint. Both nonlinear and linearized case of the diode characteristic was considered. For the linearized case two methods were used in order to validate the procedure and to find the best (and fast) variant of reaching the results. When the nonlinear characteristic was considered the results obtained in our study were compared to those offered by the commercial software SPICE. Also a comparative analysis was made between the converter's linear and nonlinear circuit. All the obtained results proved the correctness of our approaches and their concordance with the converter theory and with similar results published in the technical literature.

Unlike previous works our study is focused mainly on the circuit analysis of the step-down dc-dc converter mentioned in electromagnetic compatibility studies, offering alternative methods for its approach. It makes a detailed analysis and suggests some algorithms to study the behavior of the converter using time analysis methods.

The explanations that accompany the results tried to bring out some electric circuit specific issues, but they suggest also some advantages and disadvantages of the numerical integration procedures.

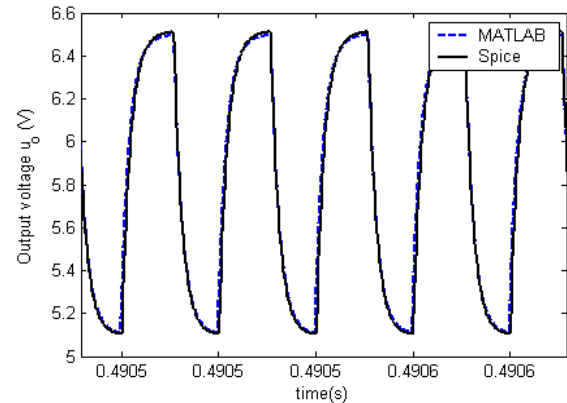


Fig. 28. The load voltage u_o in steady state for the duty ratio of 0.5 and using the nonlinear characteristic of the diode (MATLAB result versus SPICE result).

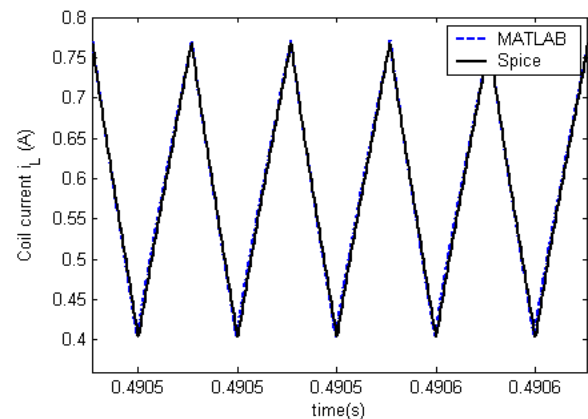


Fig. 29. The coil current i_L in steady state for the duty ratio of 0.5 and using the nonlinear characteristic of the diode (MATLAB result versus SPICE result).

This analysis on the step-down dc-dc converter as linear and nonlinear circuit wanted to bring a contribution and to complete the theoretical studies made on this subject. Thus our study can be successfully used in practice also through the obtained results but particularly through the various algorithms suggested here.

ACKNOWLEDGMENT

This work was partially supported by the grant number 32C/2014, awarded in the internal grant competition of the University of Craiova.

Received on July 26, 2015

Editorial Approval on November 21, 2015

REFERENCES

- [1] M. Rashid, *Power Electronics Handbook*. Canada: Academic Press, 2001.
- [2] B. Williams, *Power Electronics - Devices, Drivers, Applications and Passive Components*, University of Strathclyde, Glasgow, IEEE print, 2006, pp.348 - 411.
- [3] E. Rondon-Pinilla, F. Morel, C. Vollaie, and J. L. Schanen, "Modeling of a buck converter with a SiC JFET to predict EMC conducted emissions", *IEEE Transactions on Power Electronics*, vol. 29, no. 5, p. 2246-2260, May 2014.
- [4] J. J. Chen, B. H. Hwang, C. M. Kung, W. Y. Tai, and Y. S. Hwang, "A new single-inductor quadratic buck converter using

- average-current-mode control without slope-compensation", *the 5th IEEE Conference on Industrial Electronics and Applications*, 15-17 June 2010, Taichung, p. 1082 – 1087.
- [5] M. Veerachary and V. Jain, "Analysis of zero-voltage transition fourth-order buck converter", *2014 International Conference on Advances in Energy Conversion Technologies*, 23-25 January 2014, Manipal, India, p. 152 – 157.
- [6] B. Wu, J. Yang, J. Wang, and S. Li, "Extended state observer based control for dc-dc buck converters subject to mismatched disturbances", *33rd Chinese Control Conference*, 28-30 July 2014, Nanjing, China, p. 8080-8085.
- [7] I. D. Nicolae, I. G. Sirbu, D. G. Stănescu, and P. M. Nicolae, "Theoretical and practical aspects concerning the dc driving system on a tram", *National Symposium of Theoretical Electrotechnics SNET 2007*, 12-14 October 2007, Bucharest, Romania, pp 535-540.
- [8] M. Iordache and L. Dumitriu, *Modern Theory of Electric Circuits (Teoria moderna a circuitelor electrice)*, vol. II, Bucharest: ALL Educational, 2000.
- [9] J. Mahadavi, A. Emaadi, M. D. Bellar, and M. Ehsani, "Analysis of power electronic converters using the generalized state-space averaging approach", *IEEE Transactions on Circuits and Systems*, vol. 44, no. 8, p. 767-770, August 1997.
- [10] J. Xu and C.Q. Lee, "Generalized state-space averaging approach for a class of periodically switched networks", *IEEE Transactions on Circuits and Systems*, vol. 44, no. 11, p. 1078-1081, November 1997.
- [11] R. Filc, "Equivalents method for linear circuits transients calculation", *Proceedings of the International Conference on Modern Problems of Radio Engineering, Telecommunications and Computer Science*, 2002, p. 18-23.
- [12] L. Mandache, *Computer Assisted Analysis of the Electric Circuits (Analiza asistata de calculator a circuitelor electrice)*. Craiova: Sitech, 2004.
- [13] M. Iordache, L. Mandache, M. Perpelea, *Numerical Analysis of the Nonlinear Analogic Circuits (Analyse numérique des circuits analogiques non linéaires)*. Marseille: Groupe Horizon, 2006.
- [14] I. G. Sirbu, M. Voinea, and M. Iordache, "The circuit analysis of a step-down dc-dc converter under ideal and real passive components assumption", *2014 International Conference on Applied and Theoretical Electricity*, 23-25 October 2014, Craiova, Romania, p.1-5.
- [15] M. Ghinea, V. Fireteanu, *MATLAB (MATLAB - Calcul numeric, grafica, aplicatii)*. Bucharest: Teora, 2003.
- [16] L. O. Chua and P. M. Lin, *Computer-Aided Analysis of Electronic Circuits - Algorithms and Computational Techniques*, New Jersey: Prentice-Hall, Inc., 1975.
- [17] L. O. Chua, C. A. Desoer, and E. S. Kuh, *Linear and Nonlinear Circuits*, New York: McGraw-Hill Book Company, 1987.
- [18] J. Vlach, A. Opal, "Modern CAD methods for analysis of switched networks", *IEEE Transactions on Circuits and Systems*, vol. 44, no. 8, p. 759-762, August 1997.
- [19] P. M. Nicolae and M. Voinea, "Modeling and simulation of electromagnetic conducted emissions from buck converter with resistive load", *Annals of the University of Craiova, Electrical Engineering series*, no. 36, pp.154-157, 2012.
- [20] C.R. Paul, *Introduction on Electromagnetic Compatibility*, 2nd ed., New York: Wiley, 2006.
- [21] H. W. Ott, *Electromagnetic Compatibility Engineering*, New York: Wiley, 2009.